DIVISION OF BRAIN BIOLOGY †

Professor
YAMAMORI, Tetsuo

Associate Professor
WATAKABE, Akiya

Assistant Professor:	*KOMINE, Yuriko*
	SADAKANE, Osamu
NIBB Research Fellow:	*OHTSUKA, Masanari**
Technical Staff:	*OHSAWA, Sonoko*
Postdoctoral Fellow:	*TAKAJI, Masafumi*
	OHTSUKA, Masanari
	HATA, Katsusuke
	NAKAGAMI, Yuki
SOKENDAI Graduate Student:	*SHUKLA, Rammohan*
Technical Assistant:	*NAKAMURA, Tohru*
	MORITA, Junko
	IMAI, Akiko
	KON, Yayoi

This year we have reported the following results. (1) Distribution of serotonin receptor subtypes and serotonergic terminations in the marmoset brain, (2) Simultaneous visualization of extrinsic and intrinsic axon collaterals in the mouse brain, (3) Characterization of claustral neurons, (4) Distinct motor impairments of dopamine D1 and D2 receptor knockout mice.

I. Distribution of serotonin receptor subtypes and serotonergic terminations in the marmoset brain

We examined the mRNA expression patterns of all the 13 members of the serotonin receptor (5HTR) family, by *in situ* hybridization (ISH) and the distribution of serotonergic terminations by serotonin transporter (SERT) protein immunohistochemical analysis. Ten of the 13 5HTRs showed significant mRNA expression in the marmoset brain. Our study showed several new features of the organization of serotonergic systems in the marmoset brain. (1) The thalamus expressed only a limited number of receptor subtypes compared with the cortex, hippocampus, and other subcortical regions. (2) In the cortex, there is layer-selective and area-selective mRNA expression of 5HTRs (Figure 1). (3) Highly localized mRNA expressions of 5HT1F and 5HT3A were observed. (4) There was a conspicuous overlap of the mRNA expression of receptor subtypes known to have somatodendritic localization of receptor proteins with dense serotonergic terminations in the visual cortex, the central lateral (CL) nucleus of the thalamus, the presubiculum, and the medial mammillary nucleus of the hypothalamus. This suggests a high correlation between serotonin availability and receptor expression at these locations. (5) The 5HTRs show differences in mRNA expression patterns between the marmoset and mouse cortices whereas the patterns of both the species were very similar in the hippocampus. We discussed the possible roles of 5HTRs in the marmoset brain revealed by the analysis of their overall mRNA expression patterns (Published in Front. Neural Circuits, 19 May 2014 | doi: 10.3389/fncir.2014.00052).

II. Simultaneous visualization of extrinsic and intrinsic axon collaterals in Golgi-like detail for mouse corticothalamic and corticocortical cells: a double viral infection method

We reported a novel tracing technique to stain projection neurons in Golgi-like detail by double viral infection. We used retrograde lentiviral vectors and adeno-associated viral vectors (AAV) to drive the "TET-ON/TET-OFF system" in neurons connecting two regions (Figure 2).

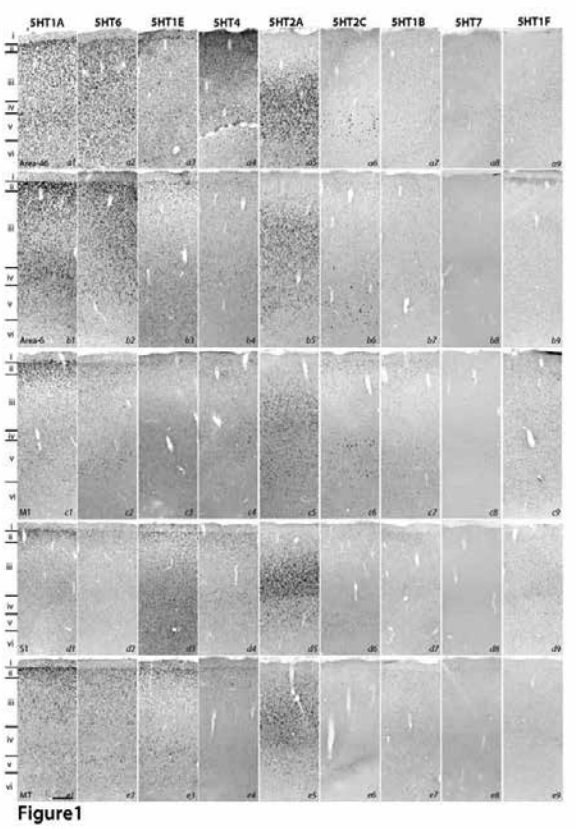

Figure1

Figure 1. ISH expression profiles of 5HTRs in the cortex. Area 46, area 6, primary motor cortex (M1), primary somatosensory cortex (S1), and V5 (MT). Layers identified by Nissl staining (not shown) are indicated on the left. Note that all images of a given gene are grouped together and presented at the same contrast level. Scale bar: 100 μm. (Cited from Shukla et al., Front. Neural Circuits, 8: 52, 2014).

Using this method, we successfully labeled the corticothalamic (CT) cells of the mouse somatosensory barrel field (S1BF) and motor cortex (M1) in their entirety (Figure 3). We also labeled contra- and ipsilaterally-projecting corticocortical (CC) cells of M1 by targeting contralateral M1 or ipsilateral S1 for retrograde infection. The strength of this method is that we can observe the morphology of specific projection neuron subtypes en masse. We found that the group of CT cells extended their dendrites and intrinsic axons extensively below but not within the thalamorecipient layer in both S1BF and M1, suggesting that the primary target of this cell type is not layer 4. We also found that both ipsi- and contra-lateral targeting CC cells in

Note: Those members appearing in the above list twice under different titles are members whose title changed during 2014. The former title is indicated by an asterisk (*).
†: This laboratory was closed on 31 March, 2015.

M1 commonly exhibit widespread collateral extensions to contralateral M1 (layers 1–6), bilateral S1 and S2 (layers 1, 5 and 6), perirhinal cortex (layers 1, 2/3, 5, and 6), striatum, and claustrum. These findings not only strengthened the previous findings of single cell tracings but also extended them by enabling cross-area comparison of CT cells or comparison of CC cells of two different labeling systems (Published in Watakabe et al., Front. Syst. Neurosci. 8: 110, 2014).

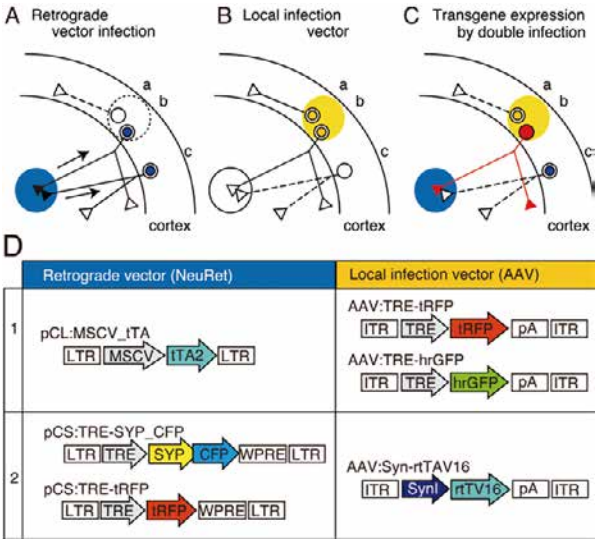

Figure 2. Schematic view of the TET double infection strategy and the viral vector constructs used for the experiments. (A–C) Schematic view of our double infection method, which utilizes the TET system. In this scheme, AAV is injected into the cortex (represented by yellow shading) as the local infection vector, while the NeuRet vector is injected into the subcortical region (represented by blue shading) as the retrograde vector. These vectors contain either tTA or TRE-transgene as depicted in **(D)**. In these panels, three neurons indicated as "a," "b," and "c" are shown. In panel **(A)**, the neurons infected with the retrograde vector ("b" and "c") are indicated by blue nuclei. The arrows represent the retrograde transport of the viral particles. In **(B)**, the neurons infected with the local infection vector ("a" and "b") are indicated by yellow nuclei. Panel **(C)** shows the consequence of double infection. Since the tTA and TRE-transgene are both present in neuron "b," high-level expression of the transgene takes place and fills the entire neuron with the transgene product (represented by red coloring). No transgene expression occurs when the neurons are infected by only one of the two viral vectors (e.g., neurons "a" and "c"). **(D)** Schematic representations of the viral constructs we used in this study. CFP, celulean; SynI, human synapsin I promoter; SYP, synaptophysin; tTA2, "TET-Off" tetracyclin transactivator; rtTV16, "TET-ON" reverse tetracyclin transactivator; tRFP, turboFP635; LTR, long terminal repeat; ITR, inverted terminal repeat; TRE, tetracycline responsive element; pA, poly(A) site; WPRE, woodchuck hepatitis virus post-transcriptional regulatory element (Cited from Watakabe et al., Front Neural Circuits. 8:110, 2014).

III. Characterization of claustral neurons by comparative gene expression profiling and dye-injection analyses

We investigated the identity of the claustrum as a part of the cerebral cortex, and in particular of the adjacent insular cortex, by connectivity features and patterns of gene expression. We mapped the cortical and claustral expression of several cortical genes in rodent and macaque monkey brains (*nurr1, latexin, cux2, and netrinG2*) to further assess shared features between the cortex and the claustrum. In

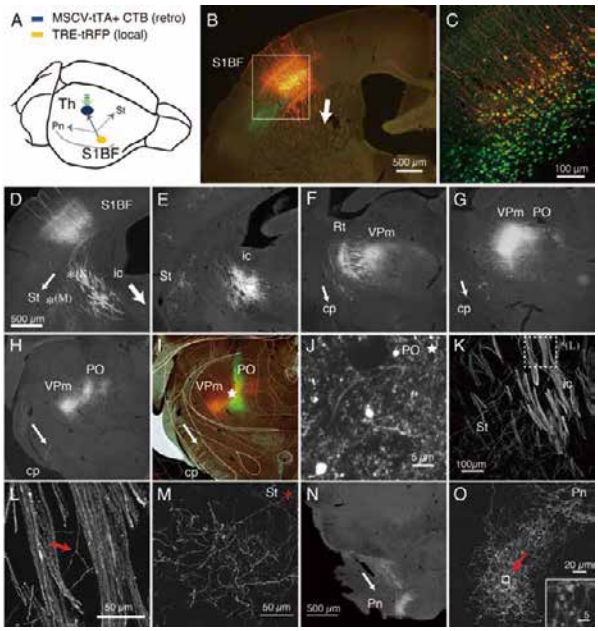

Figure 3. The identity of the claustrum as a part of the cerebral cortex, CT cells were efficiently labeled by TET

(A) Schematic view of double injection. The NeuRet vector encoding tTA (MSCV_tTA) was injected into the thalamus (represented by the green arrow) as a retrograde vector, together with CTB-Alexa488. The AAV vector carrying TRE-tRFP was injected into S1BF. We observed collateral projections to the thalamus (Th), striatum (St) and pons (Pn). (B) The coronal section at the level of S1BF showing CT cells that were labeled red by expression of tRFP. The green signals are also CT cells retrogradely labeled by CTB-Alexa488. The arrow indicates the direction of corticothalamic projections.

(C) Magnified view of the white square in (B). The contrast of this confocal image is adjusted so that we can identify each labeled cell body. (D–I) Coronal images of the tRFP signals that follow those in (B) were aligned in order from anterior to posterior. The arrows indicate the directions of the collateral projections labeled by this strategy. (D) The striatal collateral splits at the level of (D) [*(K) and *(M); higher magnification views in (K,M)]. In (E–H), the thalamic projection that proceeded in the internal capsule (ic) innervate reticular thalamic nucleus (Rt), VPm and PO, while the split collaterals proceed within the cerebral peduncle (cp). (I) Multicolor merged view for (H), which is just around the thalamic injection site. The green signals indicate the local deposit of CTB-Alexa 488, which mark the injection center for the retrograde vector. The asterisk shows the position of (J). The Paxinos atlas (Paxinos and Franklin, 2003) was superimposed to the image in (H) to make (I), to show the identification of the spots of concentrated tRFP signals. (J) A magnified view of the injection site indicated by asterisks in (I). Note that we can examine the fine branches with boutons even around the injection site (K) A magnified view of the striatal collaterals that branched out of the CT bundles of internal capsule (see D for low magnification view). The dotted square [denoted as *(L)] is magnified in (L) to indicate the example of collateral branching (indicated by the red arrow). (M) A magnified view of the striatal collaterals that arborized at the final destination (see D for low magnification view). (N) A low power view of the pontine collaterals. (O) A magnified view of the terminal arborization of pontine collaterals. The boxed region indicated by a red arrow is magnified in the inset, which exhibits a cluster of large boutons. The images used in (C, J–O) are maximal projection stacks of confocal sections.

Definitions: S1BF, somatosensory barrel field; Th, thalamus; Pn, pons; St, striatum; ic, internal capsule; cp, cerebral peduncle; Rt, reticular thalamic nucleus; VPm, ventral posteromedial nucleus; PO, posterior thalamic nuclear group (Cited from Watakabe et al., Front. Neural Circuits *8*:110, 2014).

mice, these genes were densely expressed in the claustrum, but very sparsely in the cortex and not present in the striatum. To test whether the cortical vs. claustral cell types

can be distinguished by co-expression of these genes, we performed a panel of double ISH in mouse and macaque brains. NetrinG2 and nurr1 genes were co-expressed across the entire cortex and claustrum, but cux2 and nurr1 were co-expressed only in the insular cortex and claustrum. Latexin was expressed, in the macaque, only in the claustrum. The nurr1+ claustral neurons expressed VGluT1, a marker for cortical glutamatergic cells and send cortical projections. Taken together, our data suggest a partial commonality between claustral neurons and a subtype of cortical neurons in the monkey brain. Moreover, in the embryonic (E110) macaque brain, many nurr1+ neurons were scattered in the white matter between the claustrum and the insular cortex, possibly representing their migratory history. In a second set of experiments, we injected Lucifer Yellow intracellularly in mouse and rat slices to investigate whether dendrites of insular and claustral neurons can cross the border of the two brain regions. Dendrites of claustral neurons did not invade the overlying insular territory. In summary, the gene expression profile of the claustrum is similar to that of the neocortex, in both rodent and macaque brains, but with modifications in density of expression and cellular co-localization of specific genes (Published in Watakabe, et al., Front Syst Neurosci. 8:98, 2014).

IV. Distinct motor impairments of dopamine D1 and D2 receptor knockout mice revealed by three types of motor behavior

We examined the behavioral difference among N10 congenic D1R and D2R KO, and wild type (WT) mice. Both D1R and D2R knock out (KO) mice of the major dopamine receptors show significant motor impairments. However, there are some discrepant reports, which may be due to differences in genetic background and experimental procedures. In addition, only a few studies directly compared the motor performance of D1R and D2R KO mice. First, we examined spontaneous motor activity in the home cage environment for 5 consecutive days. Second, we examined motor performance using the rota-rod task, a standard motor task in rodents. Third, we examined motor ability with the Step-Wheel task in which mice were trained to run in a motor-driven turning wheel adjusting their steps on foothold pegs to drink water. The results showed clear differences among the mice of three genotypes in three different types of behavior. In monitoring spontaneous motor activities, D1R and D2R KO mice showed higher and lower 24 h activities, respectively, than WT mice. In the rota-rod tasks, at a low speed, D1R KO mice showed poor performance but later improved, whereas D2R KO mice showed good performance early, without further improvement. When first subjected to a high speed task, the D2R KO mice showed poorer rota-rod performance at low speeds than the D1R KO mice. In the Step-Wheel task, across daily sessions, D2R KO mice increased their running speed sufficiently to reach the waterspout, and decreased time between touching the floor due to missing the peg, and decreased the number of times the wheel was stopped, which was much better performance than that of D1R KO mice. These incongruent results between the two tasks for D1R and D2R KO mice may be due to differences in motivation for the rota-rod and Step-Wheel tasks, i.e. aversion- and reward-driven, respectively. The Step-Wheel system may become a useful tool for assessing the motor ability of WT and mutant mice (Published in Nakamura et al., Front Integr. Neuroscience. 8: 56, 2014).

Publication List

〔Original papers〕

- Nakamura, T., Sato, A., Kitsukawa, T., Momiyama, T., Yamamori, T., and Sasaoka, T. (2014). Distinct motor impairments of dopamine D1 and D2 receptor knockout mice revealed by three types of motor behavior. Front. Integr. Neurosci. *8*, 56.
- Shukla, R., Watakabe, A., and Yamamori, T. (2014). mRNA expression profile of serotonin receptor subtypes and distribution of serotonergic terminations in marmoset brain. Front. Neural Circuits *8*, 52.
- Watakabe, A., Ohsawa, S. Ichinohe, N., Rockland, K.S., and Yamamori, T. (2014). Characterization of claustral neurons by comparative gene expression profiling and dye-injection analyses. Front. Syst. Neurosci. *8*, 98.
- Watakabe, A., Takaji, M., Kato, S., Kobayashi, K., Mizukami, H., Ozawa, K., Ohsawa, S., Matsui, R., Watanabe, D., and Yamamori T. (2014). Simultaneous visualization of extrinsic and intrinsic axon collaterals in Golgi-like detail for mouse corticothalamic and corticocortical cells: a double viral infection method. Front. Neural Circuits *8*, 110.

〔Original paper (E-publication ahead of print)〕

- Watakabe, A., Ohtsuka, M, Kinoshita, M. Takaji, M. Isa, K Mizukami, H., Ozawa, K. Isa, T., and Yamamori, T. Comparative analyses of adeno-associated viral vector serotypes 1, 2, 5, 8 and 9 in marmoset, mouse and macaque cerebral cortex. Neurosci. Res. 2014 Sep 18.